JOURNAL OF Materials CHEMISTRY

Cs_4C_{60}: single phase synthesis and orientational order

Patrik Dahlke, Paul F. Henry and Matthew J. Rosseinsky*†

Inorganic Chemistry Laboratory, Department of Chemistry, University of Oxford, South Parks Road, Oxford, UK OX1 3QR

Cs_4C_{60} is reported as a pure phase for the first time, using low-temperature synthesis. It adopts an orthorhombic distortion of the body-centred tetragonal (bct) A_4C_{60} structure found for K_4C_{60} and Rb_4C_{60}, due to the orientational ordering of the C_{60}^{4-} anions with the 6:6 bonds directed along the orthorhombic *b*-axis. The caesium cations occupy two distinct distorted tetrahedral sites, producing the orientational order to avoid close contact with the five-membered rings of neighbouring C_{60}^{4-} anions. The structure-directing influence of large cations on fulleride structures and the implications for Jahn–Teller distortions of the fulleride anions are discussed.

Introduction

The intercalation compounds of the most abundant fullerene C_{60} attract attention due to their wide range of electronic properties.[1] Orientational and positional disorder are seen as increasingly important variables in controlling fulleride electronic structure.[2] Although superconductivity has not been observed in C_{60}^{4-} fullerides, the structural chemistry and unusual electronic properties of the body centred tetragonal A_4C_{60} phases[3] have resulted in continued interest in these materials. Of particular importance is the absence of metallic behaviour in the formally 2/3 filled t_{1u} band, in contrast to the superconducting, metallic A_3C_{60} phases in which the t_{1u} band is 1/2 filled. Experimental investigations using photoelectron spectroscopy (PES),[4] NMR and magnetisation,[5] muon spin relaxation (μSR)[6] and Raman scattering[7] indicate that the ground states of these compounds are non-magnetic with small-gap (30–100 meV) semiconductivity below 480 K (the different estimates may refer to co-existing indirect and direct gaps). The insulating behaviour has been assigned to density waves formed due to Fermi surface nesting effects,[8] to electron repulsion producing a Mott–Hubbard insulator,[9] to the effects of orientational disorder[10] and to a Jahn–Teller distortion resulting in the formation of a low-spin state in which the lower two orbitals are fully occupied.[11] However, metallic behaviour is predicted by high-level band structure calculations on orientationally ordered structures.[8] NMR measurements show the development of a Korringa-like term under pressure, indicating that a metal–insulator transition occurs at pressures beyond 8 kbar, although there is no superconductivity at 15 kbar above 0.4 K, despite a similar value of $N(E_f)$ to that found for K_3C_{60}.[11] Recent Rietveld analysis demonstrated[9] that the K_4C_{60} and Rb_4C_{60} phases are line phases with well defined compositions, leading to the suggestion that the precisely stoichiometric composition could explain the observed narrow gap semiconductivity on the basis of a Mott–Hubbard gap in a strongly correlated system.

The relation between cation size, fulleride sphere packing and anionic orientational order is critical in controlling fulleride electronic properties[1,12] and has been investigated in detail for Na, K and Rb fullerides. However, caesium fullerides have been less widely investigated. The large size of the caesium cation will produce a strong competition between metal–fulleride and fulleride–fulleride interactions in determining the orientational state of the anion. Cs_1C_{60} is a stable phase, in contrast to K_1C_{60}, due to the good cation size match with the face-centred cubic (fcc) octahedral site. Cs_3C_{60} has only recently been reported.[13] The increased size of the Cs cation drives a transition from fcc A_3C_{60} (A = K, Rb) to body-centred packing of the fulleride array and two co-existing body-centred cubic (bcc) and body-centred tetragonal (bct) phases are found at this composition. Cs_3C_{60} has the highest superconducting transition temperature yet observed for a fulleride (40 K under 12 kbar pressure), but is metastable with respect to disproportionation into Cs_1C_{60} and Cs_4C_{60}. The required low temperature synthesis of Cs_3C_{60} makes detailed structural characterisation difficult, so the influence of the large Cs^+ cation on the fulleride orientational order is unknown.

Cs_4C_{60} is not as well studied as the lighter analogues K_4C_{60} and Rb_4C_{60}, detailed investigation being hampered by the absence of a route to pure phases. The original report of the phase involved its identification as a tetragonal material, isostructural to the other A_4C_{60} phases, in a multiphase sample of nominal composition Cs_3C_{60}.[3] Subsequent reports have also been on multiphase materials prepared by solid-state routes.[14] EPR measurements[15] indicate that Cs_4C_{60} is an insulator, obeying the Curie–Weiss law with a paramagnetic moment of 0.7 μ_B per C_{60} molecule and a small antiferromagnetic interaction ($\Theta = -5$ K). ^{13}C NMR measurements show that the structure and dynamics of Cs_4C_{60} are quite different from the potassium and rubidium analogues, with several inequivalent carbon sites resolvable at room temperature.[14] It is therefore timely to devise a route to phase-pure Cs_4C_{60} and report the detailed crystal structure of this phase.

In this paper we show that, in agreement with the differences reported in the ^{13}C MAS NMR spectra, the structure of Cs_4C_{60} is, surprisingly, quite different from that of K_4C_{60} and Rb_4C_{60}. X-Ray analyses of the latter phases[9,16] indicate that the anions are orientationally disordered in space group *I*4/*mmm*, occupying two 'standard' orientations with the molecular mirror planes (cutting through the pentagon-connecting 6:6 bonds) aligned with the {1 0 0} mirror planes of the space group, *i.e.* the anion orientations in the *ab* plane are similar to those found in K_3C_{60}.[17,18] Here we show that this disorder is suppressed in Cs_4C_{60}—the C_{60}^{4-} anions are orientationally ordered with the 6:6 bonds in the *ab* plane directed along the shorter *b*-axis of the orthorhombic unit cell. This demonstrates that cation size can affect fulleride anion orientational order as well as fulleride sphere packing, producing a change from a disordered to an ordered array of the same fulleride orientations. This contrasts with the structural transition between K_3C_{60} and the Na_2AC_{60} phases[19,20] where the small sodium cation changes only the fulleride setting angle. This hitherto unsuspected influence of the large caesium cation on orientational order has implications for the structure of both components of biphasic, $T_c = 40$ K Cs_3C_{60},[13] and the relation-

†E-mail: matthew.rosseinsky@chem.ox.ac.uk

ship between the crystallographic point symmetry of the C_{60}^{4-} anion and its electronic structure.

Experimental

Cs_4C_{60} was prepared by reaction of sublimed C_{60} (50 mg, 0.0694 mmol) with Cs metal (36.9 mg, 0.2776 mmol) in liquid ammonia (distilled from sodium *via* a dual-manifold vacuum line) at $-78\,^{\circ}C$ for one hour in an H-cell. During the reaction of the solvated Cs with the C_{60} the latter dissolves, giving a clear colourless solution from which the black product precipitates. CHN analysis gives the composition of the precipitate as $Cs_4NH_3C_{60}$ [N = 1.02 (1.10)%, C = 54.93 (56.78)%, H = 0.53 (0.24)%, calculated values in parentheses]. This agrees with the weight loss upon deammoniation $\Delta m_{exp} = 0.9(2)\%$ ($\Delta m_{calc} = 1.3\%$). The ammonia was removed by distillation and the remaining solid heated at 120 °C under 10^{-5} Torr for eight hours to remove coordinated ammonia. The solid was then sealed in a Pyrex tube under 10^{-5} Torr and heated to 350 °C for five days with one intermediate regrinding. X-Ray powder diffraction data were collected on samples sealed in 0.5 mm X-ray capillaries. Initial characterisation of phase purity was performed with Cu-Kα_1 radiation on a Siemens D5000 instrument with a linear 6° position sensitive detector. Data collected on the 9.1 transmission geometry powder diffractometer at the SRS, Daresbury Laboratory were used for Rietveld refinement. Two histograms from $5 \leqslant 2\theta/^{\circ} \leqslant 25$ and $25 \leqslant 2\theta/^{\circ} \leqslant 40^{\circ}$ were collected with a counting time of 2 s per 0.02° step, spanning a total *d*-spacing range of 5.72–0.77 Å. The wavelengths of 0.997718 and 0.998428 Å were calibrated using a silicon standard prior to data collection. Rietveld refinement was performed using the GSAS suite of programs[21] with a pseudo-Voigt peakshape function and a seven term and a four term shifted Chebyshev polynomial background function for the lower and higher angle histograms respectively. Raman measurements were carried out using a Dilor LABRAM spectrometer with a HeNe laser ($\lambda = 632.817$ nm) at 20 mW power sampling a spot size of 50 μm^2.

Results

Both X-ray and Raman data indicate that synthesis in liquid ammonia[22] readily affords pure Cs_4C_{60} at low temperature. The Raman spectrum (Fig. 1) of Cs_4C_{60} features four strong lines, arising from the $H_g(1)$, $H_g(2)$, $A_g(1)$ and $A_g(2)$ intramolecular vibrations. The highest frequency mode is the tangential 'pentagonal pinch' $A_g(2)$ phonon, which remains at a constant 1438(1) cm^{-1} during all stages of the annealing process. The $A_g(2)$ mode softens at 6.2 cm^{-1} per transferred electron in K_xC_{60}, giving an expected value of 1440 cm^{-1} for Cs_4C_{60}, consistent with the observed frequency. This indicates a high degree of phase purity in the final product, with no sign of contamination from other Cs_xC_{60} phases. The absence of significant evolution of the Raman spectrum on annealing indicates the ready formation of largely amorphous $(NH_3)Cs_4C_{60}$ in the initial reaction between C_{60} and caesium dissolved in liquid ammonia. (Fig. 1) The radial $A_g(1)$ mode is observed at 493 cm^{-1}, consistent with the charge-independence of this mode frequency found for other fulleride anions.[10] The full-width-at-half-maximum (FWHM) of the $A_g(2)$ mode is 13 cm^{-1}, much larger than the 5 cm^{-1} for the radial $A_g(1)$ mode and for $A_g(2)$ in pristine C_{60}. However, both peaks can be fitted as single symmetrical Lorentzian lines, and not as Gaussians, indicating that inhomogenous broadening from a random distribution of defects is not significant.

The radial $H_g(1)$ and $H_g(2)$ modes (at 263 and 405 cm^{-1} respectively) exhibit Breit–Wigner–Fano lineshapes.[24] A fit of eqn. (1),[25]

$$I = I_{bg} + I_0\left[1 + \left(\frac{\omega-\omega_0}{q\Gamma}\right)^2 \Big/ \left\{1 + \left(\frac{\omega-\omega_0}{\Gamma}\right)\right\}^2\right] \qquad (1)$$

where Γ is the FWHM of the phonon-only Lorentzian and $q \propto T_p/T_e$ measures the coupling of the continuum (scattering rate T_e) to the single-phonon excitation (scattering rate T_p), to the $H_g(1)$ and $H_g(2)$ peaks [the values for the $H_g(2)$ mode are given in parentheses] (Fig. 2), gives the coupling constants $q = -3.78(7)$ [$-3.20(3)$], decoupled mode frequencies $\omega_0 = 264.28(5)$ [411.35(9)] cm^{-1} and width parameters $\Gamma = 4.79(6)$ [16.1(1)] cm^{-1}. The negative values of q indicate that the coupling takes place to a lower lying continuum. The values are even smaller than $q = -4.5(3)$ for $H_g(1)$ in K_3C_{60}.[25] For $q \to \infty$ a Lorentzian lineshape results.

The downshift of these modes relative to pristine C_{60} is comparable to the other A_4C_{60} phases and, especially for the strongly broadened $H_g(2)$, is much smaller than found in A_3C_{60}, presumably due to the influence of electron–phonon coupling to the delocalised carriers in the metallic C_{60}^{3-} phase. This is consistent with the interpretation of Cs_4C_{60} as a small-gap semiconductor. The width of $H_g(1)$ (11 cm^{-1}) has not increased significantly from C_{60}, in contrast to 17 cm^{-1} in A_4C_{60} (A = K, Rb).[10] However, the 35 cm^{-1} FWHM of the $H_g(2)$ vibration is larger than found for this mode in K_3C_{60} (27 cm^{-1}) and A_4C_{60} (27 cm^{-1}). For the further reduced Cs_6C_{60} phase, the lineshape of all the Raman-active vibrations returns to a narrow Lorentzian profile with some line splitting due to the lowering of symmetry from C_{60}.[26]

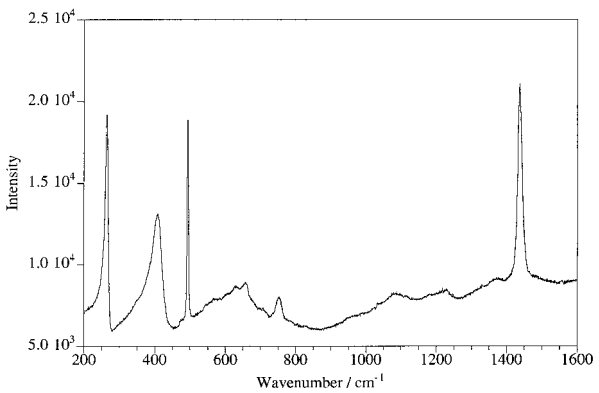

Fig. 1 Raman spectrum of Cs_4C_{60}

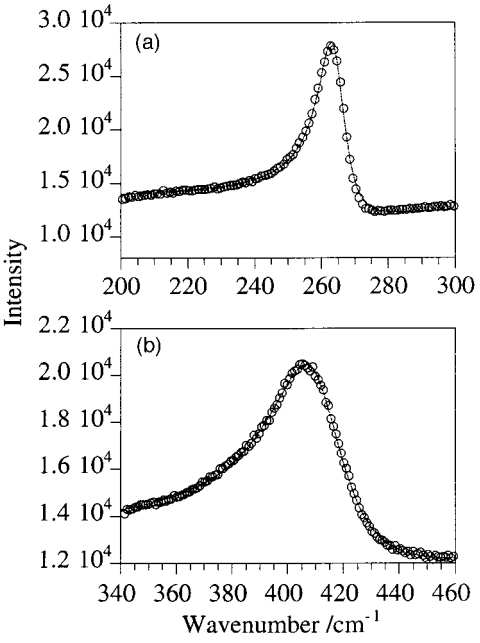

Fig. 2 The Raman modes $H_g(1)$ (a) and $H_g(2)$ (b) of the C_{60}^{4-} anion in Cs_4C_{60}. The lines correspond to fits to the Fano lineshape [eqn. (1)].

The $H_g(3)$ and $H_g(4)$ modes are broad but clearly visible at 706 and 754 cm^{-1}. $H_g(7)$ and $H_g(8)$ are broadened out as in K_4C_{60}, Rb_4C_{60} and A_3C_{60} (A = K, Rb). This overall picture is similar to that found for K_4C_{60} and Rb_4C_{60}[10] except for some reduction of intensity of the $A_g(2)$ peak relative to the rest of the spectrum and the increased width of the $H_g(2)$ mode. The additional scattering at the higher energy end of the broad overlapping region between 500 and 800 cm^{-1} has been attributed to disorder-induced scattering in the lighter A_4C_{60} phases.[10]

Inspection of the laboratory X-ray powder diffraction data indicated that Cs_4C_{60} is not isostructural with the tetragonal A_4C_{60} (A = K, Rb) phases. Initial Rietveld refinements of the synchrotron data used the body-centred tetragonal structure, adopted by the other A_4C_{60} phases and assigned from a multiphase sample in the original report of Cs_4C_{60}.[10] These refinements were unsatisfactory. The splitting of the {310}, {301}, {200} and {400} reflections (Fig. 3) indicated a lowering of the metric symmetry of the cell from tetragonal to orthorhombic. No extra Bragg reflections other than those produced by the orthorhombic splitting of allowed tetragonal reflections were observed and therefore the systematic absences within *mmm* Laue symmetry were consistent with *Immm* and its non-centric subgroups *Im*2*m*, *I*2*mm* and *Imm*2. The loss of the fourfold rotation axis along [001] can be achieved by removing the disorder in the C_{60}^{4-} orientation found in K_4C_{60} and Rb_4C_{60} by aligning the 6:6 bonds in the *ab* plane with either the orthorhombic *a* or *b* axis. Refinement clearly indicates that the 6:6 bonds perpendicular to *c* are aligned along the orthorhombic *b* axis, which is the shorter axis. The quality of the refinement was greatly improved, in particular the fit to the reflections which split on lowering the symmetry to orthorhombic. Carbon positions (Table 1) were generated by assuming the geometry of the C_{60}^{4-} anion in this case was the same as that of the C_{60}^{3-} anion (determined by powder neutron diffraction) in K_3C_{60}.[18] Refinements with 1.40 ± 0.005 Å (6:6) and 1.45 ± 0.005 Å (6:5) restraints on the C–C distances produced only a marginal improvement in the fit, suggesting both that the initial anion geometry is not significantly in error and that X-ray powder diffraction over this *d*-spacing range is not very sensitive to the details of the anion geometries, in contrast to its pronounced sensitivity to orientational order. The final Rietveld refinement is shown in Fig. 4 and the refined parameters and agreement indices are given in Table 1. Comparison of the agreement indices from the model-independent Le Bail intensity extraction[27] and the Rietveld refinement indicate that the structural model is correct. Attempts to incorporate the known Cs_6C_{60}, Cs_3C_{60} and Cs_1C_{60} phases as second phases in the refinements led to phase fractions of less than 1%, consistent with the phase purity indicated by the Raman measurements. The largest deviations in the final difference Fourier map are $\rho = +0.332$ e^- $Å^{-3}$ and $\rho = -0.258$ e^- $Å^{-3}$. The height of the positive peak corresponds to approximately 8% C ($\rho_{obs} = 5$–3.5 e^- $Å^{-3}$) or $<1\%$ Cs ($\rho_{obs} = 50$–52 $e^-Å^{-3}$).

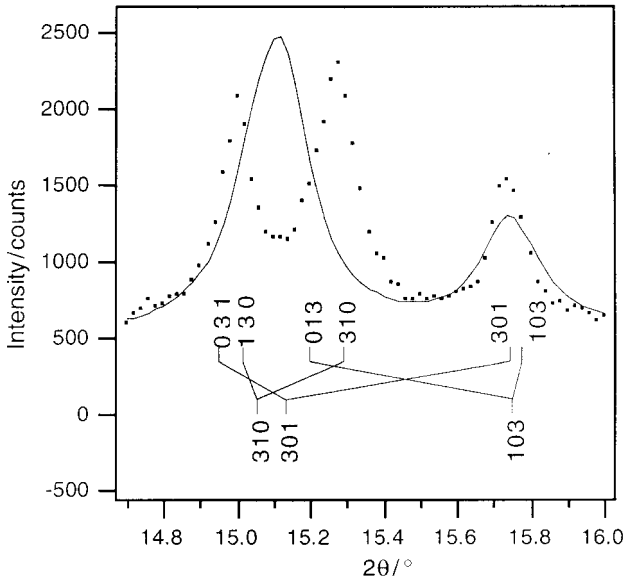

Fig. 3 Synchrotron X-ray powder diffraction reveals the lower symmetry of Cs_4C_{60}. The splitting of the Bragg reflections on lowering the symmetry from *I*4/*mmm* (lower set of Miller indices) to *Immm* (upper set of Miller indices) is indicated. The continuous line shows the best fit possible in *I*4/*mmm*.

Reduction of the symmetry to *Immm* produces two inequivalent caesium cation sites. The positional parameters of these sites refined smoothly and independently, suggesting that the space group identification was correct. No improvement was obtained by allowing anisotropic cation displacements. The difference in temperature factor between the two sites remains if the site occupancies are refined independently: the occupancies of both sites refine to the same value of 0.98(2) within the 3σ error quoted, without significantly improving the fit. Reduction of the space group symmetry to *Imm*2, *Im*2*m*, *I*2*mm*, *I*222 or *I*2/*m* allows static displacement of the caesium cations from the mirror planes. Refinements in these space groups diverged, indicating that the cations are located on the mirror planes and the *Immm* space group is correct.

Discussion

The Raman data and synchrotron X-ray Rietveld refinement show that the synthesis of pure Cs_4C_{60} by the liquid ammonia route[22] is possible, proceeding *via* an ammonia-containing intermediate which precipitates directly from the solution. This is in contrast with published reports using vapour phase intercalation and may be related to slow diffusion of caesium in the solid state although more definitive experiments on this point are required. The insolubility of the C_{60}^{4-} precursor may avoid kinetic trapping at the stable $x = 1$ and $x = 6$ phases in attempted solid state syntheses of Cs_4C_{60}.

The distinction between Cs_4C_{60} and its lighter homologues is the orientational order of the C_{60}^{4-} anions. The A_4C_{60} structure[3] can be considered as a cation-ordered derivative of the $Im\bar{3}$ A_6C_{60} structure in which the tetragonal *c*-axis is defined by the ordering of cation vacancies onto the 4d site in *I*4/*mmm*. The *c*/*a* ratio increases with increasing A^+ radius, from 0.906 (K) *via* 0.921 (Rb) to 0.952 (Cs).

Three views of the orthorhombic orientationally ordered structure of Cs_4C_{60} are shown in Fig. 5. In the *I*4/*mmm* structure of K_4C_{60} and Rb_4C_{60}, the anions are disordered over two mirror-related 'standard' orientations with the 6:6 bonds in the *ab* plane oriented equally along *a* and *b*. Fig. 5(i) shows the alignment of the 6:6 bond along the orthorhombic *b*-axis, which produces a contraction of the unit cell in this direction. The cation vacancy ordering seen in the anion-disordered structures is retained, as shown in Fig. 5(ii) and (iii). The anion orientational order produces two distinct caesium cation sites, shown in Fig. 6.

In the orientationally disordered *I*4/*mmm* structure, each of the four anions neighbouring the pseudo-tetrahedrally coordinated A cation (which occupies only one crystallographically distinct site) coordinates to it 50% *via* a six-ring and 50% *via* a five-ring. The orientation with the five-ring would therefore approach as close to the cation as an orientation coordinating *via* a six-ring. In Cs_4C_{60}, the caesium cations occupy two distinct distorted tetrahedral sites (Cs1 2*mm*, Cs2 *m*2*m*) with respect to the orientationally ordered C_{60}^{4-} anions, approaching two pentagons and two hexagons in an ordered manner. This differs from the tetrahedral sites in the K_3C_{60} structure,[17,18] where the tetrahedral cation neighbours the six-membered rings on the four surrounding anions. In Cs_4C_{60}, the cations approach closer

Table 1 Parameters and agreement indices derived from the Rietveld analysis of two histograms of synchrotron powder X-ray diffraction data on Cs_4C_{60}. Wavelengths and refined zero-point errors for both histograms are quoted. The positions and temperature factors of the carbon atoms in the C_{60}^{4-} anion were fixed in the final refinements quoted here, after constrained refinement indicated that they were not detectably displaced from the initial positions

	wR_p	R_p	R_{F^2}			x	y	z	U_{iso}/Å^2
$\lambda = 0.997718$ Å, $\Delta_{2\theta} = -0.002(2)°$	5.11	4.02	—	LeBail extraction histogram 1	C1	0.2875	0.0000	0.0608	0.01
					C2	0.2497	0.0996	0.1247	0.01
$\lambda = 0.997718$ Å, $\Delta_{2\theta} = -0.0017(8)°$	6.03	4.82	2.94	Rietveld refinement histogram 1	C3	0.2131	0.1943	0.0630	0.01
					C4	0.0573	0.2935	0.0000	0.01
$\lambda = 0.998428$ Å, $\Delta_{2\theta} = -0.0026(2)°$	3.46	2.74	1.57	Rietveld refinement histogram 2	C5	0.1175	0.2548	0.1035	0.01
					C6	0.0594	0.2175	0.2020	0.01
					C7	0.0000	0.0585	0.3051	0.01
$\chi^2 = 2.120$, 28 variables	4.83	3.66	2.13	Indices for combined Rietveld refinement of histograms 1 and 2	C8	0.0976	0.1199	0.2649	0.01
					C9	0.1904	0.0606	0.2261	0.01
					Cs1	0.2446(3)	0.5000	0.0000	0.018(3)
					Cs2	0.5000	0.2051(3)	0.0000	0.009(3)

$a = 12.1496(9)$, $b = 11.9051(9)$, $c = 11.4520(9)$ Å, $V = 1656.4(3)$ Å^3.

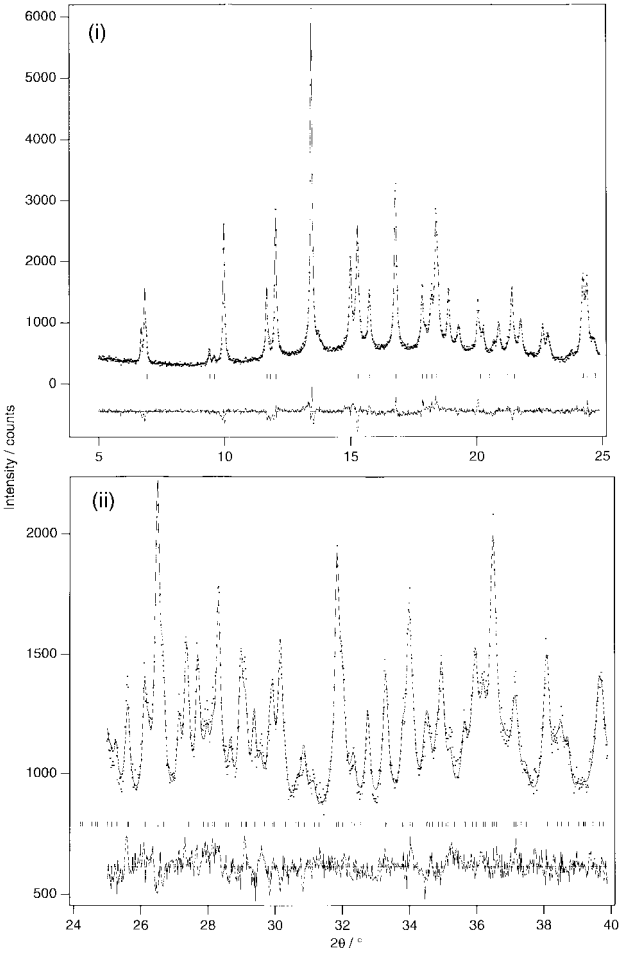

Fig. 4 Rietveld refinement of synchrotron X-ray powder diffraction data collected on Cs_4C_{60}. (i) Histogram 1, (ii) histogram 2. The observed data are denoted by square data points, the calculated and difference plots are shown as solid lines. Ticks mark the positions of the Bragg reflections. The parameters and agreement indices for this Rietveld refinement are given in Table 1.

to the C_{60}^{4-} anions which coordinate *via* the six-membered ring. The distances from Cs1 to the centres of the two fulleride neighbours coordinating *via* the six-ring are 6.51 Å while the two five-ring neighbours are at 6.66 Å; in the case of Cs2 the distances are 6.55 Å and 6.72 Å respectively. If the alternative anion orientation, with the 6:6 bond parallel to *a* in the *ab* plane, was present in the *Immm* structure, unfavourable Cs···C contacts as short as 3.11 Å would occur to carbon atoms in the five-membered ring from the fulleride located at a Cs···C_{60} distance appropriate to coordination *via* a six-ring. A direct comparison with the *I*4/*mmm* disordered structures adopted by K_4C_{60} and Rb_4C_{60} can be made by calculating distances in a tetragonal Cs_4C_{60} structure with an average *a* parameter of 12.0273 Å, giving a closest Cs···C contact of 3.15 Å. The adoption of the orientationally ordered structure here is thus driven by the larger size of the caesium cation, giving an interesting contrast with the influence of the small sodium cation on fulleride anion orientation.[1,12]

Constrained refinement showed that X-ray diffraction was not sensitive to any small displacements of the carbon atoms away from the initial anion geometry generated from that of C_{60}^{3-}. Mean Cs···C distances to neighbouring rings on the fulleride anions, calculated from the rigid anion positions, are therefore used to discuss the structure. The local environments of the two distinct caesium cations are similar on average, as judged by the mean Cs···C separations of approximately 3.58 Å in both cases (Table 2). As the closest C···K contacts in K_3C_{60} are 3.20 Å, these distances are consistent with the expected increase in ionic radius from 1.33 to 1.70 Å. However, the cation coordination is less regular in the present case. The more regularly coordinated Cs2 cation lies almost directly above the centroids of the rings [Fig. 6(ii)], while Cs1 [Fig. 6(i)] is significantly displaced from this symmetrically coordinated position towards one or two of the carbons in each five- or six-membered ring respectively. The regularity of the differing coordinations can be quantified by considering the angle through which the vector from the caesium cation to the centroid of the ring is tilted away from the ring normal (Table 2). The small tilt angles for Cs2 (below 2°) contrast with the significant displacement of Cs1 towards the C9–C9′ bond of the coordinating six-ring and the C4 atom of the nearest pentagons. The distinct differences in the spread of distances between the two sites, while retaining the same mean distance opens up the possibility of interesting substitutional chemistry in this structure.

The structure adopted by Cs_4C_{60} is a direct subgroup of the orientationally ordered $Im\bar{3}$ structure of Cs_6C_{60}. Extra anion orientational disorder is present in both the A_4C_{60} and the A_3C_{60} (A = K, Rb) phases in contrast with their A_6C_{60} parents. The A15 structure with space group $Pm\bar{3}n$, adopted by Ba_3C_{60},[28] is another ordered cation vacancy derivative of the A_6C_{60} structure which, like Cs_4C_{60}, also retains ordered C_{60} molecules. To establish a space group relationship between A_6C_{60} and A15 one has to move up the Bärninghausen tree from $Im\bar{3}$ to $Im\bar{3}m$ and down again to $Pm\bar{3}n$. The idealised cation site in $Im\bar{3}m$ is 12d. This splits on the k_2 transition into 6c and 6d, of which 6c is occupied by Ba in Ba_3C_{60} and 6d remains vacant. The coordination of C_{60} to barium, *via* the five-membered rings only, contrasts with the two five-ring and two six-ring neighbours of the caesium cation in Cs_4C_{60}.

The clear decrease in orientational disorder from K_4C_{60} and Rb_4C_{60} makes the interpretation of the Raman spectrum of

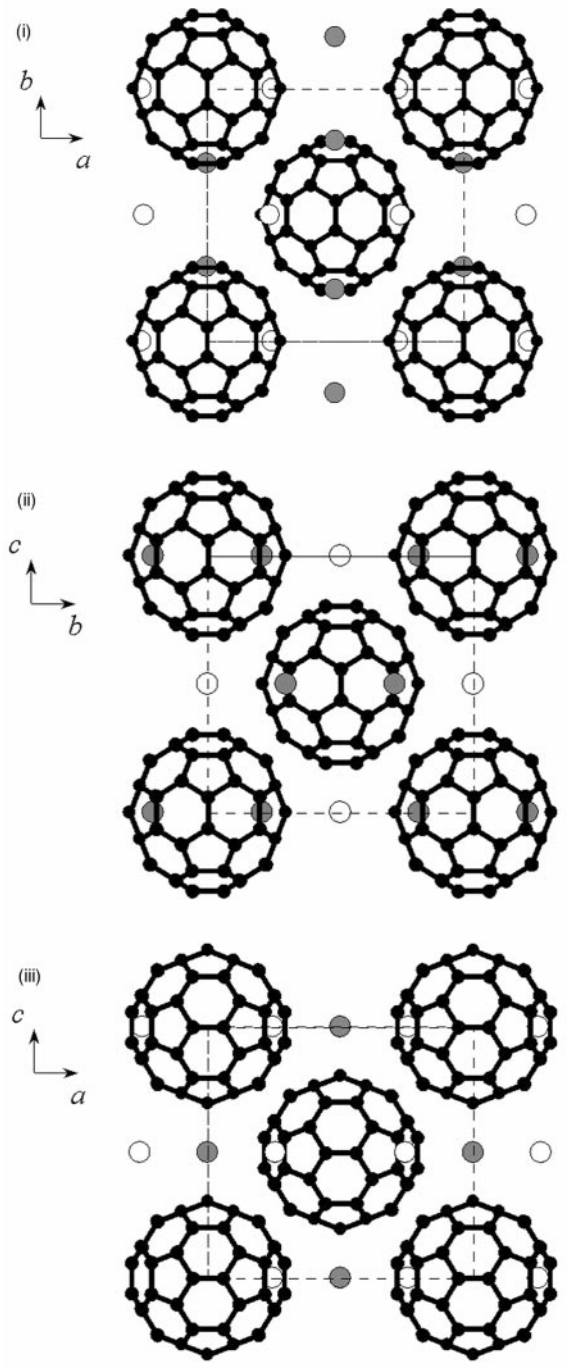

Fig. 5 The orientationally ordered *Immm* structure of Cs_4C_{60}. The Cs1 cation is unshaded, Cs2 is shown as grey and carbon atoms are black. (i) View along the [001] axis, showing the orientation of the 6:6 bond along the orthorhombic *b*-axis. The ordering of the cation vacancies is shown in the *bc* (ii) and *ac* (iii) planes.

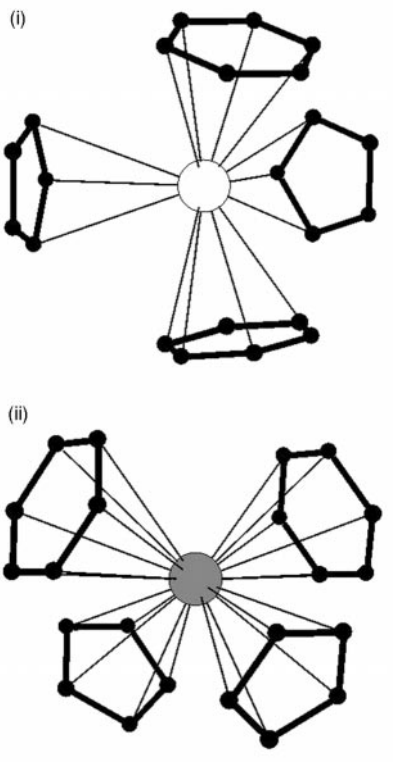

Fig. 6 A view of the coordination of (i) Cs1 and (ii) Cs2 cations to the two neighbouring six-membered rings and two neighbouring five-membered rings from the nearest C_{60}^{4-} anions. Cs···C contacts of less than 3.63 Å are indicated by solid lines.

Table 2 A summary of distances (Å) showing the different interactions of the two distinct caesium cation sites with the neighbouring C_{60}^{4-} anions. The number in brackets following the mean Cs···C distance is the standard deviation from this mean, indicating the regularity of the coordination. The use of the tilt angle (°) of the Cs···ring centroid vector from the plane normal is described in the text

mean Cs1···C distance for five-membered ring	3.56(14)
Cs1···five-ring centroid distance	3.35
tilt from ring normal towards C4	10.5
mean Cs1···C distance for six-membered ring	3.60(25)
Cs1···6-ring centroid distance	3.31
tilt from ring normal towards C9–C9′	20.8
mean Cs2···C distance for five-membered ring	3.603(6)
Cs2···centroid distance	3.38
tilt from ring normal towards C7	0.6
mean Cs2···C distance for six-membered ring	3.59(3)
Cs2···centroid distance	3.29
tilt from ring normal towards C3–C3′	1.2

Cs_4C_{60} important, as several features of the A_4C_{60} (A = K, Rb) Raman spectrum have been assigned to the influence of disorder.[10] The two lowest frequency H_g modes display the Fano lineshape, which arises from coherent Raman scattering by a phonon and a continuum of excitations. This lineshape is often observed in heavily doped semiconductors due to interband or other transitions within extended states.[29] In K_3C_{60}, Fano lineshapes were explained by a strong coupling between the discrete Raman active gerade modes and the Jahn–Teller split $t_{1u} \rightarrow t^*_{1u}$ continuum,[30] while resonant Raman scattering has offered evidence for a similar low-lying continuum produced by Jahn–Teller splitting of the C_{60}^{4-} ground state.[7] It has however been argued that overlapping of lines produced by lifting of mode degeneracies on symmetry reduction may give a lineshape closely resembling the Fano one.[31] Coupling to a continuum of Cs-related multi-phonon states[25] could also produce the observed Fano shape. This will be stronger for those vibrations with a high degree of radial character, such as the $H_g(2)$ mode, whose motion is 90% radial.[32] This has precedent in detailed studies of Fano lineshapes in the graphite intercalation compound CsC_8, where interaction with a low-lying continuum of Cs···C multiphonon excitations was demonstrated.[33] The shape of the Fano resonance in the present case indicates that the continuum extends to lower energy than either phonon mode. In view of the persistence of this lineshape in the present orientationally well ordered material, the continuum-coupled Fano resonance or symmetry-lowering mode-splitting models have more validity than disorder-induced radial mode scattering. The enhanced

broadening of the H_g radial modes and the excess scattering in the 6–800 cm^{-1} region found for K_4C_{60} and Rb_4C_{60} are both maintained in the well ordered Cs_4C_{60}, suggesting the above origins, rather than anion orientational disorder alone, for the appearance of the Raman spectra of these phases.

Conclusion

The *Immm* structure of Cs_4C_{60} accounts for the observation of several distinct resonances in the ^{13}C NMR signal from this phase.[14] This is due to the inequivalent carbon sites in the orientationally ordered and slowly reorientating C_{60}^{4-} anions. The anion 6:6 bonds are aligned along the orthorhombic *b*-axis by the close Cs···C contacts, which also slow the jump reorientation of the fulleride sufficiently (90° jumps around the *c*-axis will be strongly disfavoured for reasons discussed above) to allow observation of distinct ^{13}C resonances, rather than a single motionally narrowed line. This orientational ordering, in the same structure where the smaller alkali cations produce disorder, has important consequences for the electronic properties of this and other caesium fullerides. The highest T_c in fulleride systems is found in a mixture of bcc and bct Cs_3C_{60}, with the bct phase assigned a defect A_4C_{60} structure.[13] The present results imply that the bct component is orientationally ordered, and that the anion ordering in both phases will differ from the Ba_3C_{60} type. The local orientational order is likely to be of the *Immm* type, with the broad diffraction lines resulting from the low temperature synthesis disguising a small orthorhombic distortion.

Available EPR[15] and NMR[14] data and recent EELS measurements[34] suggest that, like its lighter analogues, Cs_4C_{60} is non-metallic. The similarity of the Raman spectrum presented here with those of K_4C_{60} and Rb_4C_{60}, compared with the clear differences seen in Raman spectra of insulating Na_3C_{60} and metallic K_3C_{60},[35] also indicate that Cs_4C_{60} is a semiconductor. This suggests that orientational disorder *per se* is not a key ingredient in the insulating behaviour of the A_4C_{60} phases, re-focussing attention on Mott–Hubbard and Jahn–Teller origins for the gap. In all the A_4C_{60} phases, the Jahn–Teller distortion required to lift the orbital degeneracy of the C_{60}^{4-} anion requires symmetry lowering away from $m\bar{3}$, in which the t_{1u} degeneracy is maintained. It is important to note that 4/*mmm* is not a subgroup of $m\bar{3}$ (C_{60} has no fourfold rotational axis) and thus the $I4/mmm$ space group adopted by K_4C_{60} will only lift the orbital degeneracy through the action of the average crystal field at the anion site, rather than by inducing a Jahn–Teller distortion of the anion itself to 4/*mmm* symmetry. By contrast, the *mmm* anion symmetry in the orientationally ordered Cs_4C_{60} structure is a subgroup of $m\bar{3}$, and thus the orientational order demonstrated here is entirely consistent with Jahn–Teller distortion of the anion itself. The orientational order may thus be coupled to Jahn–Teller distortion of the anion, driven by the enhanced t_{1u} electron localisation produced by the larger interfulleride separation here compared with tetragonal Rb_4C_{60}. The t_{1u} degeneracy will be completely lifted by a distortion of the C_{60}^{4-} anion to *mmm* symmetry. This will produce a filled band insulator at the 4− charge, removing the need to postulate a Mott–Hubbard insulating state to explain the behaviour of Cs_4C_{60}. A unifying picture for the A_4C_{60} systems is that the on-site repulsion U localises the t_{1u} electrons (indicated by quantitative analysis of the optical gap[34]), which then produce the Jahn–Teller distortion. The synergic operation of electron–electron and electron–phonon coupling appears to produce an unusual Mott-Hubbard insulating ground state in which there are no local magnetic moments, in contrast to the well studied magnetic Mott–Hubbard insulators found in, for example, many first row transition metal oxides.

We thank the EPSRC for a studentship to P.F.H. and access to the SRS, where Dr. G. Bushnell-Wye assisted us on station 9.1. We thank the Leverhulme Trust for their continued support of this work.

Note added at proof: the superconducting alkaline earth fullerides Ba_4C_{60} and Sr_4C_{60} have recently been shown to adopt the orthorhombic distortion of the bct structure described here.[36]

References

1 K. Prassides, *Curr. Opin. Solid State Mater. Sci*, 1997, **2**, 433.
2 Y. Iwasa, *J. Phys. Chem. Solids*, 1997, **58**, 1697.
3 R. M. Fleming, M. J. Rosseinsky, D. W. Murphy, A. P. Ramirez, R. C. Haddon, T. Siegrist, R. Tycko, G. Dabbagh and C. Hampton, *Nature*, 1991, **352**, 701.
4 P. J. Benning, F. Stepniak and J. H. Weaver, *Phys. Rev. B*, 1993, **48**, 9086.
5 I. Lukyanchuk, N. Kirova, F. Rachdi, C. Goze, P. Molinie and M. Mehring, *Phys. Rev. B*, 1995, **51**, 3978.
6 R. F. Kiefl, T. L. Duty, J. W. Schneider, A. Macfarlane, K. Chow, J. W. Elzey, P. Mendels, G. D. Morris, J. H. Brewer, E. J. Ansaldo, C. Niedermayer, D. R. Noakes, C. E. Stronach, B. Hitti and J. E. Fischer, *Phys. Rev. Lett*., 1992, **69**, 2005.
7 G. Ruani, P. Guptsarma, C. Taliani and J. E. Fischer, *Physica C*, 1994, **235**, 2477.
8 S. C. Erwin and C. Bruder, *Physica B*, 1994, **199**, 600.
9 C. A. Kuntscher, G. M. Bendele and P. W. Stephens, *Phys. Rev. B*, 1997, **55**, R3366.
10 M. G. Mitch and J. S. Lannin, *Phys. Rev. B*, 1995, **51**, 6784.
11 R. Kerkoud, P. Auban-Senzier, D. Jerome, S. Brazovskii, I. Lukyanchuk, N. Kirova, F. Rachdi and C. Goze, *J. Phys. Chem. Solids*, 1996, **57**, 143.
12 J. E. Fischer, *J. Phys. Chem. Solids*, 1997, **58**, 1939.
13 T. T. M. Palstra, O. Zhou, Y. Iwasa, P. E. Sulewski, R. M. Fleming and B. R. Zegarski, *Solid State Commun*., 1995, **93**, 327.
14 C. Goze, F. Rachdi and M. Mehring, *Phys. Rev. B*, 1996, **54**, 5164.
15 H. Suematsu, Y. Murakami, T. Arai, K. Kikuchi, Y. Achiba and I. Ikemoto, *Mater. Sci. Eng. B*, 1993, **19**, 141.
16 O. Zhou and D. E. Cox, *J. Phys. Chem. Solids*, 1992, **53**, 1373.
17 P. W. Stephens, L. Mihaly, P. L. Lee, R. L. Whetten, S.-M. Huang, R. Kaner, F. Diederich and K. Holczer, *Nature*, 1991, **351**, 632.
18 K. M. Allen, W. I. F. David, J. M. Fox, R. M. Ibberson and M. J. Rosseinsky, *Chem. Mater*., 1995, **7**, 764.
19 K. Kniaz, J. E. Fischer, Q. Zhu, M. J. Rosseinsky, O. Zhou and D. W. Murphy, *Solid State Commun*., 1993, **88**, 47.
20 K. Prassides, C. Christides, I. M. Thomas, J. Mizuki, K. Tanigaki, I. Hirosawa and T. W. Ebbesen, *Science*, 1994, **263**, 950.
21 A. C. Larson and R. B. von Dreele, General Structure Analysis System, LAUR 86-748, Los Alamos National Laboratory, 1994.
22 R. P. Ziebarth, D. R. Buffinger, V. A. Stenger, C. Recchia and C. H. Pennington, *J. Am. Chem. Soc*., 1993, **115**, 9267.
23 J. Winter and H. Kuzmany, *Solid State Commun*., 1992, **84**, 935.
24 U. Fano, *Phys. Rev. B*, 1961, **124**, 1866.
25 P. C. Eklund, P. Zhou, K. A. Wang, G. Dresselhaus and M. S. Dresselhaus, *J. Phys. Chem. Solids*, 1992, **53**, 1391.
26 P. Zhou, K.-A. Wang, P. C. Eklund, M. S. Dresselhaus and R. A. Jishi, *Phys. Rev. B*, 1992, **46**, 2595.
27 A. LeBail, H. Duroy and J. L. Fourquet, *Mater. Res. Bull*., 1988, **23**, 447.
28 A. R. Kortan, N. Kopylov, S. Glarum, E. M. Gyorgy, A. P. Ramirez, R. M. Fleming, O. Zhou, F. A. Thiel, P. L. Trevor and R. C. Haddon, *Nature*, 1992, **360**, 566.
29 J. Bak, U. Venkateswaran, C. L. Mak, R. Sooryakumar and B. T. Jonker, *J. Phys. Chem. Solids*, 1995, **56**, 563.
30 T. Pichler, M. Matus and H. Kuzmany, *Solid State Commun*., 1993, **86**, 221.
31 H. Kuzmany, M. Matus, B. Burger and J. Winter, *Adv. Mater*., 1994, **6**, 731.
32 R. E. Stanton and M. D. Newton, *J. Phys. Chem*., 1988, **92**, 2141.
33 N. Caswell and S. A. Solin, *Phys. Rev. B*, 1979, **20**, 2551.
34 M. Knupfer and J. Fink, *Phys. Rev. Lett*., 1997, **79**, 2714.
35 J. S. Lannin and M. G. Mitch, in *Raman Scattering of Alkali-Metal Fullerides*, ed. K. Prassides, Kluwer Academic, Dordrecht 1994, p. 311.
36 K. Prassides, personal communication.

Paper 8/01508B; *Received* 23*rd February*, 1998